

Thermodynamic Properties of Strongly Degenerate Interacting Fermi Systems

V.S. Filinov* and M. Bonitz
Fachbereich Physik, Universität Rostock
Universitätsplatz 3, D-18051 Rostock, Germany
 (November 21, 2018)

A numerical approach is presented which allows to calculate the equilibrium properties of Fermi systems which are both, *strongly coupled and strongly degenerate*. Based on a novel path integral representation of the many-particle density operator, quantum and spin effects are included. As an illustration, results for the pressure and energy of an electron-proton plasma are presented.

Coulomb systems continue to attract the interest of researchers in many fields, including plasmas, astrophysics, solids and nuclear matter, see Refs. [1,2] for an overview. Stimulated by recent impressive experimental advances [1], theoretical activities follow a large variety of approaches: exactly solvable models [1,2], kinetic theory and quantum statistics, e.g. [3,4], computer simulations, e.g. [5–7] and others. The most interesting phenomena such as metallic hydrogen, plasma phase transition, Fermi liquids, bound states etc., occur in situations where both Coulomb *and* quantum effects are relevant. However, here, all present theories have practical difficulties. Quantum kinetic methods easily handle quantum and spin effects, but they become extremely complicated when correlation effects can not be treated perturbatively. On the other hand, Monte Carlo (MC) and molecular dynamics (MD) simulations allow for an efficient treatment of strong coupling phenomena, but still have difficulties with incorporating quantum and spin statistics effect.

In particular, there has been remarkable progress in applying path integral quantum Monte Carlo (PIMC) techniques to Bose [8] and Fermi systems, see e.g. [5–7,9] and Ref. [10] for an overview. However, there remains one major obstacle preventing efficient modelling of Fermi systems – the so-called sign problem, i.e. the appearance of differences of large numbers in the expressions for thermodynamic quantities. It is related to the antisymmetrization of the fermionic N-particle density matrix which results in a sum of $N!/2$ positive and negative terms in the thermodynamic functions. This led to a number of additional approximations, such as the fixed node and restricted path integral concepts. Despite impressive recent simulation results, see [9,10] and references therein, to overcome these assumptions remains one of the challenges from the fundamental (first principal character) as well as practical point of view.

In this work we demonstrate that these approxima-

tions can in fact be avoided. We derive a different path integral representation for the density matrix ρ by introducing a modified set of integration variables. This leads to two major advantages for the thermodynamic functions: i) they do not contain an explicit sum over permutations (with alternating sign) and ii) part of the volume and temperature dependencies of ρ can be eliminated. As an example, we present explicit formulas for the equation of state and energy of a two-component plasmas, cf. Eqs. (8) and (9). The numerical efficiency of our approach is demonstrated with results for the pressure and energy of a high-temperature/high-density electron-proton plasma over a wide range of degeneracy parameters. Our approach has important consequences for simulations of Fermi systems, such as dense quantum plasmas, few-fermion systems in traps or quantum confined semiconductor structures [11] and is the basis for developing path integral MD simulations for Coulomb systems [12].

As is well known the thermodynamic properties of a quantum system of N particles are fully determined by the partition function Z and, consequently, by the density matrix [13]

$$Z = \int_V dq \rho(q, 0; q, \beta), \quad \rho(q, \beta; q', \beta') \equiv \langle q\beta | \hat{\rho} | \beta' q' \rangle, \quad (1)$$

where $\hat{\rho} = \exp\{-(\beta - \beta')\hat{H}\}$, $\beta = 1/k_B T$, and q comprises the coordinates of all particles, $q \equiv \{\mathbf{q}_1, \mathbf{q}_2, \dots, \mathbf{q}_N\}$. With an analytical expression for the density matrix given, one can use e.g. Monte Carlo methods [5–7,10] to evaluate the partition function and thermodynamic quantities. However, for a quantum system, ρ is, in general, not known but can be constructed from its known high-temperature limit by means of a decomposition into $n+1$ factors, each of which corresponds to the density matrix at an $n+1$ times higher temperature [13],

$$\rho(q, 0; q', \beta) = \frac{1}{N!} \sum_P (\pm 1)^{\kappa_P} \int_V dq^{(1)} \dots dq^{(n)} \times \rho(q, 0; q^{(1)}, \tau^{(1)}) \dots \rho(q^{(n)}, \tau^{(n)}; \hat{P} q', \beta), \quad (2)$$

where $\tau^{(i+1)} - \tau^{(i)} = \Delta\beta = \beta/(n+1)$. Eq. (2) lets one view the N-particle state as a loop consisting of $n+1$ vertices (“beads”) located at intermediate coordinates $q^{(i)}, \tau^{(i)}, i = 1 \dots n$. For quantum systems of bosons (fermions), furthermore, in Eq. (2), the spin statistics theorem has been taken into account which requires to

perform an (anti-)symmetrization of the density matrix giving rise to the sum over all N -particle permutations P with parity κ_P , and \hat{P} denotes the permutation operator. Obviously, for fermions (minus sign in the parantheses), this sum contains $N!/2$ positive and $N!/2$ negative terms. (To simplify the notation, we have not written the spin variables explicitly, their inclusion is straightforward).

The unknown density matrix (2) is efficiently computed by approximating the ρ 's on the r.h.s. of Eq. (2) by the high-temperature density matrix ρ^{hT} . For potentials which are bounded from below, the simplest choice is, e.g. [5,6],

$$\begin{aligned} \rho^{hT}[q^{(i)}, \tau^{(i)}; q^{(i+1)}, \tau^{(i+1)}] &\approx \rho_0[q^{(i)}, \tau^{(i)}; q^{(i+1)}, \tau^{(i+1)}] \\ &\times e^{-[\tau^{(i)} - \tau^{(i+1)}]U(q^{(i)})}, \\ \rho_0[q^{(i)}, \tau^{(i)}; q^{(i+1)}, \tau^{(i+1)}] &= \frac{1}{\lambda_\Delta^{3N}} \prod_{p=1}^N e^{-\frac{\pi}{\lambda_\Delta^2} |q_p^{(i)} - q_p^{(i+1)}|^2}, \end{aligned} \quad (3)$$

where ρ_0 is the free-particle density matrix which is a product of single-particle density matrices, U is the potential energy, and λ_Δ is the DeBroglie wave length corresponding to $k_B(n+1)T = 1/\Delta\beta$, $\lambda_\Delta^2 \equiv 2\pi\hbar^2\Delta\beta/m$. It is well known that for $n \rightarrow \infty$, ρ^{hT} converges to the exact density matrix ρ . Notice that the factorization of ρ^{hT} into a kinetic and potential energy term, Eq. (3), is an approximation also. The error made thereby is of the order of the variation of U on the spatial scale λ_Δ and thus vanishes with $n \rightarrow \infty$. This holds also for a repulsive Coulomb potential, whereas the attractive electron-ion interaction has to be represented by a bounded from below effective pair potential [3,5,10,9].

After recalling the general concept of PIMC, we now explain our scheme. To simplify the presentation, we choose a binary mixture of quantum electrons and classical protons, $N_e = N_i = N$. The first crucial step is to transform the intermediate electron coordinates. To this end, we rewrite the partition function (1), now explicitly including the arguments of the ions,

$$\begin{aligned} Z(N, V, \beta) &= \frac{Q(N_e, N_i, \beta)}{N_e! N_i! \lambda_i^{3N_i} \lambda_\Delta^{3N_e}}, \\ \text{with } Q(N_e, N_i, \beta) &= \int_V dq dr d\xi \rho(q, [r], \beta). \end{aligned} \quad (4)$$

Here, the notation q is retained for the ions. $[r]$ summarizes the electron coordinates with r denoting the coordinates at the beginning of the fermionic loop and $\xi^{(1)}, \dots, \xi^{(n)}$ the dimensionless distances between neighboring vertices on the loop. Thus, explicitly, $[r] \equiv [r; r + \lambda_\Delta \xi^{(1)}; r + \lambda_\Delta (\xi^{(1)} + \xi^{(2)}); \dots]$, and $q, r, \xi^{(i)}$ each are $3N$ -dimensional vectors. For the density matrix in Eq. (4) we have, using (3), [5,14]

$$\rho(q, [r], \beta) = \sum_{s=0}^N \rho_s(q, [r], \beta) \quad (5)$$

$$= \sum_{s=0}^N \frac{C_N^s}{2^N} e^{-\beta U(q, [r], \beta)} \prod_{l=1}^n \prod_{p=1}^N \phi_{pp}^l \det |\psi_{ab}^{n,1}|_s,$$

where $U(q, [r], \beta) = U^i(q)$

$$+ \frac{1}{n+1} \sum_{l=0}^n \{U_l^e([r], \beta) + U_l^{ei}(q, [r], \beta)\}, \quad (6)$$

and U^i , U_l^e and U_l^{ei} denote the interaction energy between ions, electrons at vertex " l " and electrons (vertex " l ") and ions, respectively. Furthermore, $\phi_{pp}^l \equiv \exp[-\pi|\xi_p^{(l)}|^2]$ arises from the kinetic energy density matrix ρ_0 of the electron with index p . Notice that, in contrast to ρ_0 in Eq. (3), ϕ_{pp}^l is independent of volume and temperature. Furthermore, we underline that, in contrast to Eq. (2), Eq. (5) does not contain an explicit sum over the permutations and thus no sum of terms with alternating sign. Instead, the whole exchange problem is contained in a single exchange matrix given by

$$||\psi_{ab}^{n,1}|_s \equiv ||e^{-\frac{\pi}{\lambda_\Delta^2} |(r_a - r_b) + y_a^n|^2}|_s, \quad (7)$$

where $y_a^n = \lambda_\Delta \sum_{k=1}^n \xi_a^{(k)}$. Besides being a function of distance, this matrix contains all spin dependencies of the N -electron subsystem. The calculation of $\det|\psi_{ab}|_s$ which is crucial for evaluating the density matrix (5) is greatly simplified by its block structure (it contains two zero submatrices) which is explained in Fig. 1. As a result of the spin summation, the matrix carries a subscript s denoting the number of electrons having the same spin projection.

As a first example of applying our results (4), (5) to thermodynamic properties, we provide the result for the equation of state, $\beta p = \partial \ln Q / \partial V = [\alpha / 3V \partial \ln Q / \partial \alpha]_{\alpha=1}$,

$$\begin{aligned} \frac{\beta p V}{2N} &= 1 + \frac{1}{6NQ} \sum_{s=0}^N \int dq dr d\xi \rho_s(q, [r], \beta) \times \\ &\left\{ \sum_{p < t}^{N_i} \frac{\beta e^2}{|q_{pt}|} + \sum_{p < t}^{N_e} \frac{\beta e^2}{(n+1)|r_{pt}|} - \sum_{p=1}^{N_i} \sum_{t=1}^{N_e} \frac{|x_{pt}|}{n+1} \frac{\partial \beta \Phi^{ie}}{\partial |x_{pt}|} + \right. \\ &\sum_{l=1}^n \left[\sum_{p < t}^{N_e} \frac{\beta e^2 \langle r_{pt}^l | r_{pt} \rangle}{(n+1)|r_{pt}^l|^3} - \sum_{p=1}^{N_i} \sum_{t=1}^{N_e} \frac{\langle x_{pt}^l | x_{pt} \rangle}{(n+1)|x_{pt}^l|} \frac{\partial \beta \Phi^{ie}}{\partial |x_{pt}^l|} \right] \\ &\left. + \frac{\alpha}{\det|\psi_{ab}^{n,1}|_s} \frac{\partial \det|\psi_{ab}^{n,1}|_s}{\partial \alpha} \right\}. \end{aligned} \quad (8)$$

Here, Φ^{ie} is the effective electron-ion pair potential, α is a scaling parameter for the length, $\alpha = L/L_0$, $\langle \dots | \dots \rangle$ denotes the scalar product, and q_{pt} , r_{pt} and x_{pt} are differences of two coordinate vectors: $q_{pt} \equiv q_p - q_t$, $r_{pt} \equiv r_p - r_t$, $x_{pt} \equiv r_p - q_t$, $r_{pt}^l \equiv r_p - r_t + y_p^l$ and $x_{pt}^l \equiv r_p^l - q_t + y_p^l$. The structure of Eq. (8) is obvious: we have separated the classical ideal gas part (first term). The ideal quantum pressure in excess of the classical one and the correlation contributions are contained in the integral term, where the second line results from the ionic

correlations (first term) and the e-e and e-i interaction at the first vertex (second and third terms respectively). The third and fourth lines are due to the further electronic vertices and the explicit volume dependence of the exchange matrix, respectively. As a consequence of representation (5), the result (8) for the pressure does not contain a sum over permutations. In fact, each of the sums in curly brackets in Eq. (8) is bounded as the number of vertices increases, $n \rightarrow \infty$, which enables us to evaluate the pressure without additional approximations for the density matrix.

Other thermodynamic quantities exhibit the same favorable behavior. As a second result, we provide the formula for the energy, $\beta E = 6N/2 - \beta \ln Q / \partial \beta$

$$\begin{aligned} \beta E = 6Nk_B T + \frac{1}{Q} \sum_{s=0}^N \int dq dr d\xi \rho_s(q, [r], \beta) \times \\ \left\{ \sum_{p < t}^{N_i} \frac{\beta e^2}{|q_{pt}|} + \sum_{p < t}^{N_e} \frac{\beta e^2}{(n+1)|r_{pt}|} + \sum_{p=1}^{N_i} \sum_{t=1}^{N_e} \frac{\beta \Phi^{ie}(|x_{pt}|)}{n+1} \right. \\ + \sum_{l=1}^n \left[\sum_{p < t}^{N_e} \frac{\beta e^2}{(n+1)|r_{pt}^l|} - \sum_{p < t}^{N_e} \frac{\beta e^2 \langle r_{pt}^l | y_{pt}^l \rangle}{2(n+1)|r_{pt}^l|^3} \right. \\ \left. + \sum_{p=1}^{N_i} \sum_{t=1}^{N_e} \frac{\beta^2 \langle x_{pt}^l | y_p^l \rangle}{2(n+1)|x_{pt}^l|} \frac{\partial \beta \Phi^{ie}(x_{pt}^l)}{\partial |x_{pt}^l|} \right. \\ \left. + \sum_{p=1}^{N_i} \sum_{t=1}^{N_e} \frac{\beta \Phi^{ie}(x_{pt}^l)}{n+1} \right] - \frac{\beta}{\det|\psi_{ab}^{n,1}|_s} \frac{\partial \det|\psi_{ab}^{n,1}|_s}{\partial \beta} \Big\}, \quad (9) \end{aligned}$$

where we denoted $y_{pt}^l \equiv y_p^l - y_t^l$. The structure of this result is similar to that for the pressure, Eq. (8). Again, each sum in the parantheses is bounded for $n \rightarrow \infty$.

Besides their advantageous analytical properties, expressions (8) and (9) are well suited for numerical evaluation using Monte Carlo techniques. For a fast generation of a sequence of N -particle configurations (Markov chain) [6,5] it is necessary to efficiently compute the ratio R of two exchange determinants corresponding to subsequent configurations of the Markov chain, $R = \det|\psi_{ab}^{n,1}|_{new} / \det|\psi_{ab}^{n,1}|_{old}$. The probability of accepting a MC configuration is proportional to the absolute value of R while the sign of the determinants is included in the weight function of each configuration. Without going into details we only mention that this can be done using the inverse of the exchange matrix. Moreover, the inverse matrix is used for an efficient computation of the derivatives of the exchange determinants in Eqs. (8) and (9) which is expressed in standard manner as a sum of N determinants involving derivatives of $\psi_{ab}^{n,1}$, Eq. (7).

To demonstrate our numerical scheme, we consider as an example a two-component electron-proton plasma. For the potential Φ^{ie} we chose a simple approximation of the Kelbg potential which is the high-temperature limit, of the exact electron-ion interaction, e.g. [3,14]. Thus, by increasing the number of electronic vertices n , in principle, any desired accuracy can be achieved. To simplify

the computations, we included only the dominant contribution in the sum over s corresponding to $s = N/2$ electrons having spin up and down, respectively. (The contribution of the other terms is small and vanishes in the thermodynamic limit.)

As a first test of our approach, we consider a mixture of ideal electrons and protons for which the thermodynamic quantities are known analytically, e.g. [3]. Fig. 2 shows our numerical results for the pressure together with the theoretical curve. The agreement, up to values of the degeneracy parameter $\chi \equiv n\lambda^3$ as large as 5 is remarkable. Even with only $N = 32$ electrons and protons deviations are rather small. One clearly sees that increasing the number of particles (see inset of Fig. 2) improves the numerical results systematically and extends the range of applicability to larger values of χ .

Let us now turn to the case of interacting electrons and protons. We have performed a series of calculations in which the classical coupling parameter $\Gamma = (4\pi n_e/3)^{1/3} e^2 / 4\pi\epsilon_0 kT$ was kept constant while the degeneracy was varied. The results for the pressure and energy are presented in Fig. 3. One can see that for weak coupling and small degeneracy parameters, $\chi < 0.5$, exchange effects are small, and QMC simulations without exchange (open circles) are close to our results. However, with increasing χ and Γ , the deviations are growing rapidly. Even stronger are the discrepancies with analytical theories which are constructed as perturbation expansions, and thus are limited to small values of χ and Γ . Most strikingly is the decrease of the energy as a function of χ predicted by the analytical models and QMC without exchange, which is in contrast to our results which show an increase for all values of Γ . We mention that for all results shown, the maximum statistical error is about 5% and can be systematically reduced by increasing the length of the MC run. Furthermore, the accuracy is affected by the number n of vertices. In our calculations, we considered always temperatures above one Rydberg, for which we checked that it is sufficient to use $n = 6$.

In summary, we presented a new path integral representation (5) for the N -particle density matrix which does not contain an explicit summation over permutations. As a result, we were able to compute the pressure and energy of a strongly correlated plasma of degenerate electrons and classical protons without additional assumptions for the density matrix. Our numerical results demonstrate the practical feasibility of our approach and open the way to a large variety of applications including dense hydrogen, fermion systems in condensed matter, few-fermion systems in traps [11] or semiconductor nanostructures as well as to MD simulations for fermions [12].

We acknowledge support from the Deutsche Forschungsgemeinschaft (Mercator-Programm) for VSF and stimulating discussions with B. Bernu, D. Ceperley, W. Ebeling, V.E. Fortov, D. Kremp and M. Schlanges.

-
- [1] *Strongly Coupled Coulomb Systems*, G. Kalman (ed.), Pergamon Press 1998
 - [2] Proceedings of the International Conference on Strongly Coupled Plasmas, W.D. Kraeft and M. Schlanges (eds.), World Scientific, Singapore 1996
 - [3] W.D. Kraeft, D. Kremp, W. Ebeling, and G. Röpke, *Quantum Statistics of Charged Particle Systems*, Akademie-Verlag Berlin 1986
 - [4] M. Bonitz, *Quantum Kinetic Theory*, B.G. Teubner, Stuttgart, Leipzig 1998
 - [5] V.M. Zamalin, G.E. Norman, and V.S. Filinov, *The Monte Carlo Method in Statistical Thermodynamics*, Nauka, Moscow 1977 (in Russian).
 - [6] *The Monte Carlo and Molecular Dynamics of Condensed Matter Systems*, K. Binder and G. Ciccotti (eds.), SIF, Bologna 1996
 - [7] *Classical and Quantum Dynamics of Condensed Phase Simulation*, B.J. Berne, G. Ciccotti and D.F. Coker eds., World Scientific, 1998, Singapore.
 - [8] D.M. Ceperley, Rev. Mod. Phys. **65**, 279 (1995)
 - [9] C. Pierleoni, D.M. Ceperley, B. Bernu, and W.R. Magro, Phys. Rev. Lett. **73**, 2145 (1994)
 - [10] D.M. Ceperley, in Ref. [6], pp. 447-482
 - [11] A.V. Filinov, Yu.E. Lozovik, and M. Bonitz, to be published
 - [12] V.S. Filinov, in *Progress in Nonequilibrium Green's functions*, M. Bonitz (ed.), World Scientific, Singapore 2000
 - [13] R.P. Feynman, and A.R. Hibbs, *Quantum mechanics and path integrals*, McGraw-Hill, New York 1965
 - [14] V.S. Filinov, High Temperature **13**, 1065 (1975) and **14**, 225 (1976)
 - [15] J. Riemann, M. Schlanges, H.E. DeWitt, and W.D. Kraeft, in Ref. [2], p. 82

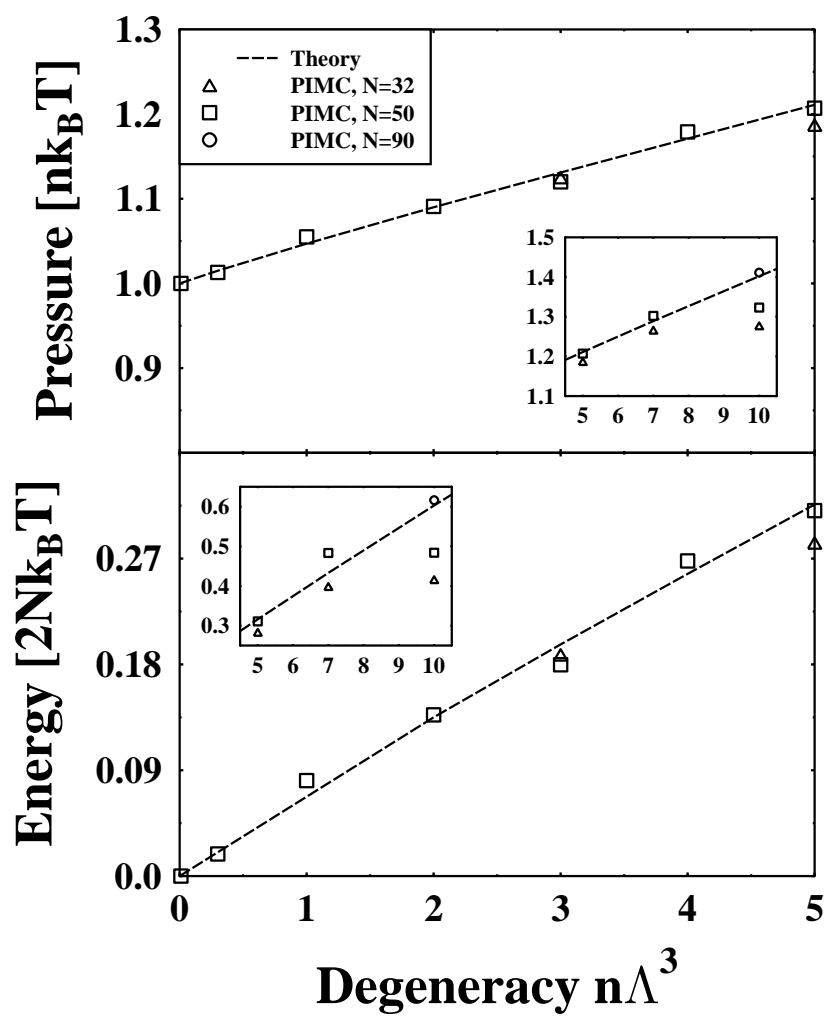
FIG. 1. Schematic of the exchange matrix $||\psi_{ab}||$. It contains two zero sub-matrices, s denotes the number of electrons with the same spin projection.

FIG. 2. Pressure (upper figure) and energy (lower figure) of an *ideal* plasma of degenerate electrons and classical proton. Theory (dashed line) is compared to PIMC simulations with varying particle number.

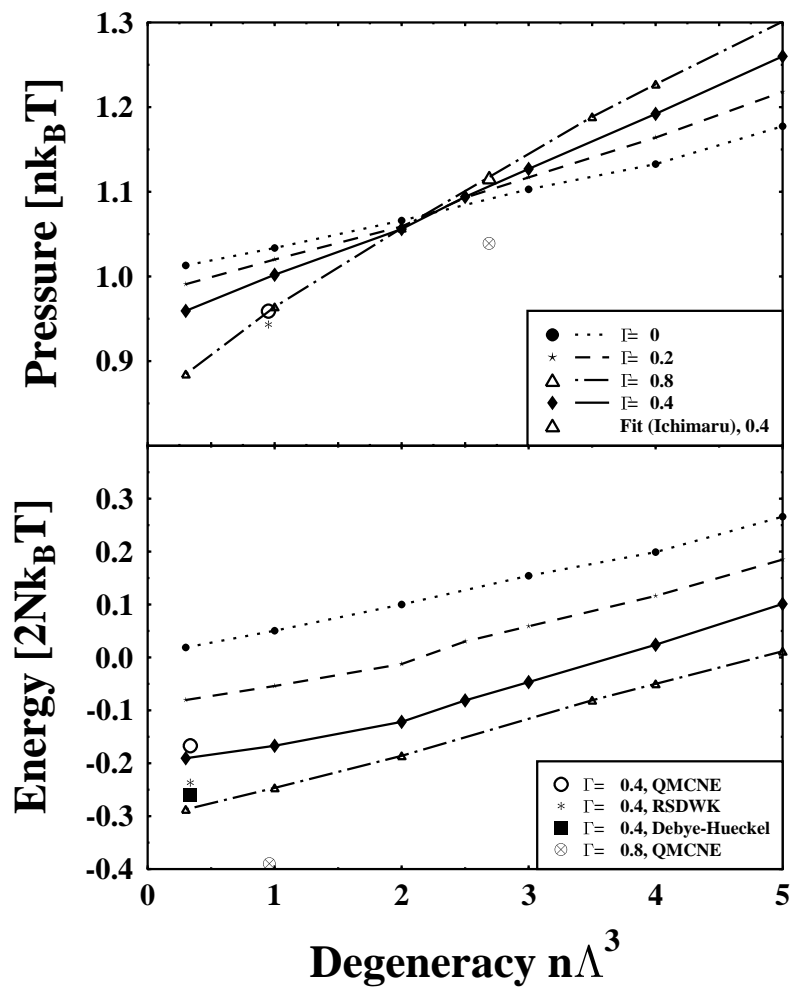
FIG. 3. Pressure (upper figure) and energy (lower figure) of a *nonideal* plasma of degenerate electrons and classical proton. Lines with symbols are PIMC simulations for different values of Γ (see inset in upper figure). Remaining symbols denote quantum MC simulations without exchange (QMCNE) and analytical models (RSDWK - quantum statistical model of Riemann et al.), data from Ref. [16].

	1	...	s	s+1	...	N
1						
⋮						
⋮						
s						
s+1						
⋮						
⋮						
N						

Filinov et al. Fig. 1



Filinov et al. Fig. 2



Filinov et al. Fig.3